0026-895X/89/010039-09$02.00/0

MOLECULAR PHARMACOLOGY, 35:39-47

Different Agonist-Receptor Active Conformations for Rat Brain M1 and M2 Muscarinic Receptors that Are Separately Coupled to Two Biochemical Effector Systems

M. MCKINNEY, D. ANDERSON, and L. VELLA-ROUNTREE

Neuroscience Research Division, Pharmaceutical Discovery, Abbott Laboratories, Abbott Park, Illinois 60064

Received May 17, 1988; Accepted October 4, 1988

SUMMARY

In dissociated cellular preparations of adult rat cortex, M1 and M2 muscarinic receptors were shown to mediate phosphoinositide metabolism and cAMP inhibition, respectively. Additionally, in dissociated striatum, an M2 receptor was shown to inhibit the level of cAMP. The components of "receptor reserve" in these three receptor-effector systems were evaluated by the method of partial receptor inactivation and the dissociation constants for the full agonist carbachol were determined. In dissociated cellular preparations of cortex, and in the presence of 10 mM lithium ion, carbachol (EC_{50} = 116 μM) activated an M1 receptor subtype (atropine K_i = 0.9 nM; pirenzepine K_i = 9.3 nM) to elicit up to a 7-fold release over the basal level of [^{3}H]inositol 1-phosphate. Carbachol was 100-fold more potent (EC_{50} ~ 1 μM) in the inhibition of forskolin-elevated [^{3}H]cAMP levels in both the cortex (maximally 28%) and striatum (maximally 49%). Pirenzepine blocked the [^{3}H]cAMP inhibition responses to carbachol in cortex and striatum with K_i values of 334 nM and 313 nM, respectively, which indicated that cortical and striatal M2 receptors mediate [^{3}H]cAMP inhibition. The equilibrium dissociation constants for the full agonist carbachol in mediating these two biochemical responses were determined after partial receptor inactivation with propylbenzilylcholine mustard. The results indicate that cortical M1 receptor-mediated phosphoinositide metabolism is elicited by carbachol through a low affinity agonist-receptor complex (carbachol K_d = 90 μM). However, the cortical and striatal M2 receptor-mediated inhibition of [^{3}H]cAMP is mediated by a high affinity agonist-receptor complex (carbachol K_d = 8.5 μM and 2.9 μM, respectively). Thus, the agonist is bound in a low affinity active conformation of the M1 receptor but the agonist is bound in a high affinity active conformation of the M2 receptor. In contrast to the cortical M1-phosphoinositide system, the central M2 receptors exhibited a significant receptor reserve in their mediation of [^{3}H]cAMP inhibition, as elicited by the full agonist carbachol. Whereas the ratio of K_d/EC_{50} for carbachol was 0.9 at the cortical M1 receptor, this ratio was 9.4 and 3.2 at the cortical M2 and striatal M2 receptors, respectively.

The pharmacological demonstration of subtypes of the muscarinic receptor has recently been corroborated by molecular cloning. Cortical M1 receptors and cardiac M2 receptors have different amino acid sequences, as deduced from their respective mRNA molecules (1–4). Further, the cloning of genomic sequences indicates that at least four intronless genes code for muscarinic receptors (5, 6). Such findings suggest numerous possibilities for tissue- and cell-specific expression of unique proteins, which would presumably couple to various effector systems. At least three of these muscarinic receptors are expressed in the cortex and hippocampus (5). Cholinergic neurotransmission via muscarinic receptors is of key importance in cortical activation (7), information processing (8, 9), and behavior (10–12). The projection from the nucleus basalis is the major source of the cortical cholinergic innervation (13) and many data support a role for this projection (e.g., see Ref. 14) and central M1 receptors (15–17) in cognitive function. However, little is rigorously known of the relationship between the specific muscarinic receptor sequences and the mechanisms of transducing ligand binding into cellular function or, ultimately, cognitive function.

Pharmacological studies of muscarinic receptor subtypes rely on the selectivity properties of pirenzepine and certain other antagonists. Studies have shown that cortical and hippocampal M1 receptors are coupled to phosphoinositide metabolism (18, 19); this class of receptor may mediate excitatory effects in cortex or hippocampus (7, 20–22). Striatal M2 receptors couple to both phosphoinositide metabolism (19) and inhibition of adenylate cyclase (18, 23). Cortical M2 receptors, thought to be in part presynaptic (24, 25), are less well characterized. Northern blot analysis indicates that the cortex expresses little or no mRNA for the cardiac type of the M2 receptor (2, 3). However, M2 binding sites are present in cortical tissue (26–28), cortical M2 receptors regulate acetylcholine release (24, 25), and an M2

ABBREVIATIONS: EC_{50}, concentration of agonist required to elicit 50% maximal response; K_i or K_b, equilibrium binding constant for an antagonist; K_d, dissociation binding constant for a ligand; pA2, negative logrithm of antagonist K_i or K_b PBS, phosphate-buffered saline; PrBCM, propylbenzilylcholine mustard.

receptor inhibits [^{3}H]cAMP levels in dissociated cortex (23). It is possible, therefore, that cortical M2 receptors are localized on the extrinsic cholinergic afferents. In the coupling to acetylcholine release modulation and the inhibition of cAMP, these cortical M2 receptors appear to be pharmacologically similar to striatal M2 receptors (23–25).

It is evident from a number of studies that agonists are more potent at central M2 receptors than at the cortical M1 receptor. For example, whereas carbachol mediates phosphoinositide metabolism in cortex with an EC_{50} value of about 100 μM (27), the EC_{50} value for this agonist in inhibiting acetylcholine release in cortical preparations (a presumptive M2 response) was about 10 μM and 1 μM (Refs. 24 and 25, respectively). The inhibition of adenylate cyclase in striatal membranes has been reported to be 1 μM or 22 μM (Refs. 26 and 18, respectively). In our studies of the cortical and striatal M2-mediated inhibition of cAMP (23), and the analogous response in N1E-115 cells (28), we observed EC_{50} values for carbachol of about 1 μM.

Such findings of greater potency for an agonist at neuronal M2 receptors suggest that these receptors may be coupled more efficiently to responses than are M1 receptors. Alternatively, the difference in EC_{50} values between M1 and M2 receptors could indicate that agonists bind selectively to M2 receptors. Although an absence of a receptor reserve in the cortical M1 receptor-mediated phosphoinositide response has been reported, the striatal M2 receptor mediating this response seems to be coupled more efficiently (27). There have been no comparable studies of the coupling efficiencies of the cortical M2 receptor, nor (to our knowledge) have there been any measures of receptor reserve in muscarinic receptor interactions with the adenylate cyclase system in brain tissue. Differences in coupling efficiencies or binding potencies of cortical M1 and M2 muscarinic receptors would have important implications for the development of selective ligands to activate or block them, particularly if they have opposing roles in setting cortical cholinergic tone.

We have found previously that accurate evaluations of ligand selectivities require the use of the same tissue preparations for both assays (29). In the present study we use dissociated rat brain preparations to demonstrate that rat cortical M1 and cortical/striatal M2 receptors, which are differentially coupled to two biochemical effector systems, bind carbachol in two different agonist-receptor conformations. Additionally, the data indicate the absence of "spareness" in the cortical M1 system but a modest receptor reserve in the M2 systems. These findings indicate that M1 and M2 receptors differ fundamentally in their recognition of agonists, provide insight into the well known phenomenon of agonist binding heterogeneity, and help to predict the effects of systemic administration of ligands on central cholinergic tone.

Methods

Preparation of dissociated brain tissue. This method of tissue preparation was originally designed for use with fetal rat brain (30) but has been employed recently for functional receptor studies in adult rat brain (23, 29, 31, 32). Cortex or striatum, dissected from adult rat (male Sprague-Dawley) brain, was mechanically dissociated, as previously described in detail (23). In brief, cortex or striatum was minced with a razor blade on an ice-cold surface, suspended in ice-cold Puck's D1 solution (138 μM NaCl, 5.4 mM KCl, 0.17 mM Na_2HPO_4, 0.22 mM KH_2PO_4, 5.5 mM glucose, and 58.4 mM sucrose; osmotic strength adjusted to 340 mOsm; pH 7.4), and filtered sequentially through two Nitex bags (210-μm and 130-μL pore). For the cAMP assays, the final suspension was washed twice with a physiological PBS solution (110 mM NaCl, 5.3 mM KCl, 1.8 mM $CaCl_2$, 1.0 mM $MgCl_2$, 25 mM glucose, 25 mM Na_2HPO_4; osmotic strength adjusted to 340 mOsm; pH 7.4). For the phosphoinositide assays, the final suspension was washed twice with oxygenated, modified Krebs-Hensleit buffer (118 mM NaCl, 4.7 mM KCl, 1.2 mM KH_2PO_4, 25 mM $NaHCO_3$, 1.3 mM $CaCl_2$, 1.2 mM $MgCl_2 \cdot 6\ H_2O$, 1.2 mM glucose). Washed dissociated tissue was suspended in PBS or Krebs-Hensleit buffer for distribution into tubes or culture wells (2–4 mg/ml final concentration). As we described previously (23), the final preparation is a mixture of dispersed cells and small fragments of brain tissue of about 100-μm diameter. Histological analysis (not shown) indicated that elements with neuronal morphology were present in this preparation.

Metabolic prelabeling of cells. For phosphoinositide assays, resuspended dissociated cortical tissue was rejuvenated with three sequential 20-min incubations in oxygenated Krebs-Hensleit buffer (composition given above) at 37° under 95% O_2/5% CO_2, with the renewal of the buffer after each incubation; the final incubation was in the presence of 10 mM lithium ion. When the effects of receptor alkylation on muscarinic receptor-mediated phosphoinositide metabolism were measured, PrBCM was added during the third 20-min incubation; this was followed by two washes with Krebs-Hensleit buffer to remove free mustard. The rejuvenated cells were then labeled 60 min at 37° in a volume of 4 ml, under an atmosphere of 95% O_2/5% CO_2, with 60 μCi of [^{3}H]inositol (New England Nuclear, Boston, MA) per rat frontoparietal cortex (two sides; approximately 260 mg total original wet weight of tissue). For cAMP assays, dispersed cells were incubated 45 min with 20–40 μCi of [^{3}H]adenine (22 Ci/mmol; Amersham, Arlington Heights, IL) at 37° in a volume of 2 ml under ambient air. For receptor alkylation studies, the mustard was incubated with tissue during the final 20 min of the [^{3}H]adenine labeling period; this was followed by two washes with PBS to remove unincorporated mustard.

Second messenger assays. For the phosphoinositide assays, the suspension of prelabeled dissociated tissue was diluted to approximately 15 mg/ml with Krebs-Hensleit buffer, containing 10 mM lithium ion, and aliquoted to 4-ml plastic tubes to a final concentration of 2–4 mg/ml. Antagonists were added and, 15 min later, agonists were added to a final volume of 300 μl; the cells were further incubated under 95% oxygen/5% CO_2 for 60 min. Reactions were terminated with the addition of 1 ml of chloroform/methanol (2:1). Chloroform (1 ml) and water (1 ml) were added to facilitate phase separation. The water contained approximately 2000 dpm of [^{14}C]inositol-1 phosphate (Amersham) as a "recovery standard." The samples were capped, vigorously mixed, and then centrifuged at 3000 rpm for 15 min to separate phases. The aqueous phases of the samples were transferred to new tubes and mixed with 2 ml of water. [^{3}H]Inositol-1 phosphate was purified on Dowex columns as previously described (33).

The [^{3}H]cAMP assays with prelabeled dissociated tissue were performed as previously described (23).

Data analysis. Concentration-response data were fitted with a four-parameter logistic model employing the program ALLFIT (34). In the studies of atropine and pirenzepine, the concentration-response curves were usually constrained to a competitive model. In the receptor occlusion experiments, the parameter values resulting from independently fitting the "control" and "treated" curves were used to calculate "smooth" values of equieffective carbachol concentrations (A, in μM for the control curve; A', in μM for the treated curve) for a range of responses in the most linear regions of the concentration-response curves. The paired inverses of A and A' were plotted and fitted by linear regression, and the slope and intercept were determined (35). The fraction of unoccluded receptors (Q) is the inverse of the slope; thus, the fractional occupany of the occluding agent is $1 - Q$. The K_d for the agonist was calculated by the following equation (35):

$$K_d = (\text{Slope} - 1)/\text{Intercept}$$

Because K_d and EC_{50} values are log-normally distributed (36), we

transformed such data (from independent experiments) to logrithmic form (i.e., obtaining pK_d and pEC_{50} values), determined the arithmetic means and standard errors of the log-transformed data, and used these to make statistical comparisons (using the unpaired Student's t test). However, data are expressed here as geometric means, i.e., as the antilogrithms of the mean pK_d or pEC_{50}. The standard error of the geometric mean was determined by multiplying the geometric mean by the standard error of the pK_d or pEC_{50} mean (37).

Results

Demonstration of the muscarinic receptor subtypes involved in cAMP and phosphoinositide metabolism in dissociated rat brain. The muscarinic receptor inhibits [^{3}H]cAMP levels in [^{3}H]adenosine-prelabeled dissociated rat cortex (23). To observe this response, we find it necessary to activate adenylate cyclase in the preparation with forskolin. A 10-min stimulation with 10 μM forskolin elevates [^{3}H]cAMP levels to a level up to 9-fold over basal; carbachol decreases the forskolin-[^{3}H]cAMP response by 20–30% (23). A composite concentration-response relation for carbachol's inhibition of the forskolin-elevated [^{3}H]cAMP levels for eight experiments in dissociated cortical tissue appears in Fig. 1, where it is compared with the concentration response for carbachol-mediated phosphoinositide metabolism in dissociated cortex. In the experiments shown, the EC_{50} for the inhibition by carbachol of the forskolin-mediated elevation of [^{3}H]cAMP levels was 1.1 ± 0.1 μM, with a maximal response at 27 ± 1.5% inhibition (eight experiments) (see Table 1).

In the [^{3}H]inositol-prelabeled dissociated cell preparation of adult rat cerebral cortex and in the presence of 10 mM lithium ion, carbachol stimulated the formation of [^{3}H]inositol-1 phosphate from 3- to 6-fold over basal levels (about twice the response we observed in 350 × 350 μm slices; data not shown). The concentration-response curve in Fig. 1 is a composite of six assays with dissociated cortical tissue (EC_{50} = 116 ± 10 μM; see Table 1 and legend to Fig. 1). In dissociated cortical tissue, atropine blocked carbachol-mediated phosphoinositide metabolism with a K_i value of 0.9 ± 0.1 nM (four experiments) and the carbachol-mediated [^{3}H]cAMP inhibition response with a K_i value of 2.7 ± 0.3 nM (four experiments). These values, which were obtained by the "dose-ratio" method, were significantly different ($p < 0.05$), indicating that atropine possesses about 3-fold selectivity for blocking cortical muscarinic receptor-mediated phosphoinositide metabolism.

Pirenzepine was employed to demonstrate which subtypes of the muscarinic receptor were involved in these two cortical responses. Pirenzepine shifted the concentration-response curves of carbachol rightward and the maximal response was achievable with higher carbachol concentrations, indicating competitive inhibition by this antagonist (Fig. 2). The cortical phosphoinositide response was inhibited potently by pirenzepine (Fig. 2A; K_i = 8 nM for the shift achieved by 30 nM pirenzepine), whereas this antagonist was much less potent in blocking the cortical [^{3}H]cAMP inhibition response to carbachol (Fig. 2B; the two K_i values were 233 nM and 417 nM, determined from the shift resulting from 10 μM and 100 μM pirenzepine). Schild plots for both cortical receptor-effector systems are shown in Fig. 3 and the data are summarized in Table 1. The $pA2$ values for pirenzepine's inhibition of the carbachol-mediated phosphoinositide and cAMP responses were 8.16 and 6.48, respectively. Because the slopes of these plots (given in the legend to Fig. 3) were not significantly different from unity, the data in Fig. 3 were constrained to unit slope in order to determine the K_b values (see Table 1). The potency of pirenzepine in blocking phosphoinositide metabolism (K_b = 9.3 nM) indicates the involvement of an "M1" receptor, whereas the potency of this antagonist in blocking the cAMP response (K_b = 334 nM) indicates mediation by an "M2" receptor.

In dissociated striatum, where carbachol elicited a potent (EC_{50} = 0.9 μM) and robust (44.6%) inhibition of 10 μM forskolin-elevated [^{3}H]cAMP levels, pirenzepine shifted the carbachol concentration-response curve rightward in accordance with competitive inhibition (Fig. 2C; K_i = 221 nM and 392 nM were calculated from the shifts achieved by 10 μM and 100 μM pirenzepine, respectively). Data for several experiments with the [^{3}H]cAMP response in dissociated striatum are plotted by the method of Arunlakshana and Schild (38) in Fig. 3; the $pA2$ for pirenzepine was 6.64. The slope of the Schild plot for this M2 response was not significantly different from unity and the calculated K_b was 313 nM (Table 1).

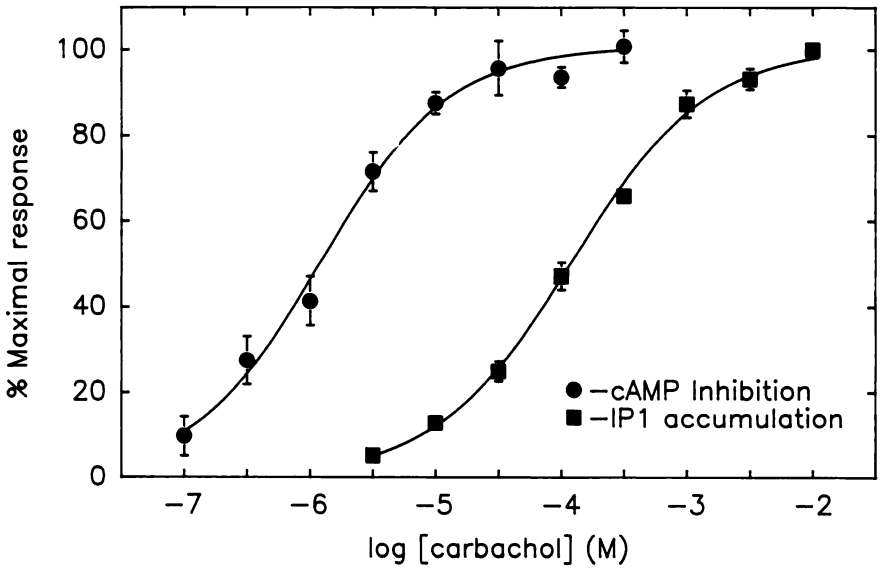

Fig. 1. Concentration-response curves for carbachol in the cortical muscarinic systems. Various concentrations of carbachol were incubated with prelabeled dispersed cortical cells. The maximal response for each experiment was normalized to 100%. The data for the inhibition of 10 μM forskolin-stimulated [^{3}H] cyclic AMP formation (●) are the averages ± standard error of eight combined experiments (100% response is 27 ± 1.7% inhibition). The data for stimulation of [^{3}H]inositol 1-phosphate (*IP1*) formation (■) are averages of six combined assays (100% response is 7537 ± 890 dpm [^{3}H]inositol 1-phosphate over basal levels, which averaged 1979 ± 237 dpm).

TABLE 1

Pharmacological properties of muscarinic receptor-mediated biochemical responses in dissociated adult rat cortex and striatum

The K_i values for atropine were calculated from the dose-ratio (DR) by the formula K_i = [antagonist]/(DR − 1). The K_i value of pirenzepine was calculated from pA2 values determined by the method of Arunlakshana and Schild (38), as described in the legend to Fig. 3, constraining the plots to have unit slopes. Numbers in parentheses, number of experiments.

Parameter	Cortex		Striatum, cAMP inhibition
	Inositol 1-phosphate formation	cAMP inhibition	
EC_{50} for carbachol (μM)	116 ± 9.9 (6)	1.12 ± 0.10 (8)	0.90 ± 0.08 (3)
Maximal response to carbachol	3.9 ± 0.4 fold[a] (6)	27.1 ± 1.5% inhibition (8)	44.6 ± 1.6% inhibition (3)
K_i atropine (nM)	0.9 ± 0.06 (4)	2.7 ± 0.3[b] (4)	ND[c]
K_i pirenzepine (nM)	9.3 ± 0.5 (6)	334 ± 21[d] (7)	313 ± 18[d] (5)

[a] Response over basal formation of [^{3}H]inositol 1-phosphate, which was 1979 ± 237 dpm (six experiments).
[b] Significantly different from K_i for inositol 1-phosphate in cortex, $p < 0.05$.
[c] ND, not determined.
[d] Significantly different from cortex inositol 1-phosphate, $p < 0.001$.

Pharmacological determination of binding constants for carbachol and measurement of receptor reserve in brain M1 and M2 receptor-effector systems. PrBCM was employed to alkylate muscarinic receptors in dissociated cortical and striatal tissue. Treatment of cortical tissue with varying concentrations of PrBCM for 20 min, followed by two washes, resulted in progressive occlusion of muscarinic receptor binding sites, as determined with [^{3}H]*N*-methylscopolamine (Fig. 4). Half-maximal occlusion with this protocol occurred with 5.6 nM PrBCM. The effect of the mustard on the concentration-response relation for carbachol was evaluated in the cortex with both the M1 and M2 responses, and in the striatum with the M2 response. Representative experiments are shown in Figs. 5–7.

Treatment of dissociated cortex with 10 nM PrBCM effected an immediate reduction of the maximal phosphoinositide response to carbachol, without increasing the EC_{50} value. In the representative experiment shown in Fig. 5, the K_d value calculated for carbachol by the method of Furchgott and Bursztyn (35) was 180 μM. As shown in Table 2, the average K_d value for five experiments with the cortical M1 receptor was 90 ± 11 μM, a value not significantly different from the average EC_{50} value for carbachol in the "control" tissue (100 ± 7 μM). The Q value (fraction of unoccluded receptors) for the experiment with the M1 receptor in Fig. 5 was 0.26, in good agreement with the value predicted from the binding data in Fig. 4, which is 0.36. In the five experiments with the cortical M1 receptor, all of which were performed with 10 nM PrBCM, the average Q value was 0.49 ± 0.07.

The method of Furchgott and Bursztyn (35) was also used to obtain the dissociation constant of carbachol for the cortical M2 receptor mediating [^{3}H]cAMP inhibition. Because of the modest response to carbachol at this receptor and the variable data obtained in treated tissue, we were able to calculate a K_d value in only three experiments. Fig. 6 shows one of these experiments, in which the K_d value for carbachol was 9.9 μM (calculated Q = 0.1; predicted Q = 0.2). The average K_d value for the three experiments was 8.5 ± 3.1 μM (Table 2). This value was significantly different from the K_d value for carbachol determined for the cortical M1 receptor ($p < 0.05$). Additionally, the K_d value of carbachol at the cortical M2 receptor was significantly higher (9.4-fold) than the corresponding EC_{50} value, indicating the presence of a substantial receptor reserve for this response.

Finally, we determined the K_d value of carbachol at the striatal M2 receptor mediating [^{3}H]cAMP inhibition. The K_d value for carbachol was 3.4 μM in the representative experiment shown in Fig. 7 (calculated Q = 0.16; predicted Q = 0.26), whereas the average K_d in five experiments with the striatal M2 receptor was 2.9 ± 0.6 uM (Table 2). This value was significantly different from the K_d for carbachol obtained for the cortical M1 receptor ($p < 0.01$) but not significantly different from the K_d for carbachol at the cortical M2 receptor. The K_d value for carbachol at the striatal M2 receptor was significantly larger (3.2-fold) than the corresponding EC_{50} value ($p < 0.05$), indicating that a receptor reserve exists for the striatal M2 system, as for the cortical M2-cAMP system.

Discussion

The primary finding of the present study is that central M1 and M2 muscarinic receptors couple with differing efficiencies to effectors for phosphoinositide metabolism (cortex) and cAMP inhibition (cortex and striatum). Our studies with dissociated cortex confirm a previous finding in cortical slices (27) of the absence of a receptor reserve in the cortical M1 receptor-effector system. In contrast, our data indicate that cortical and striatal M2 receptors involved in inhibition of cAMP levels exhibit a significant receptor reserve. The K_d/EC_{50} ratios for carbachol in the cortical and striatal M2 systems were 9.4 and 3.2, respectively. Carbachol mediated the cortical M1 response with an EC_{50} value about 100-fold greater than for the M2 responses studied and this difference in functional potency seems to be largely because the agonist binds to the M2 receptor with higher affinity (about 11-fold and 31-fold more potently to the cortical and striatal M2 receptors, respectively), as compared with the cortical M1 receptor.

Pirenzepine was about 34-fold more potent in blocking carbachol-mediated [^{3}H]inositol 1-phosphate release in dissociated cortex than in blocking carbachol-mediated [^{3}H]cAMP inhibition in dissociated cortex and striatum. Although these findings to a certain extent confirm previous work (18, 23, 26, 27), our study demonstrated this selectivity in parallel experiments using the same method of tissue preparation for the two different kinds of biochemical assays. Such comparisons using the same tissue preparation should allow more confident assess-

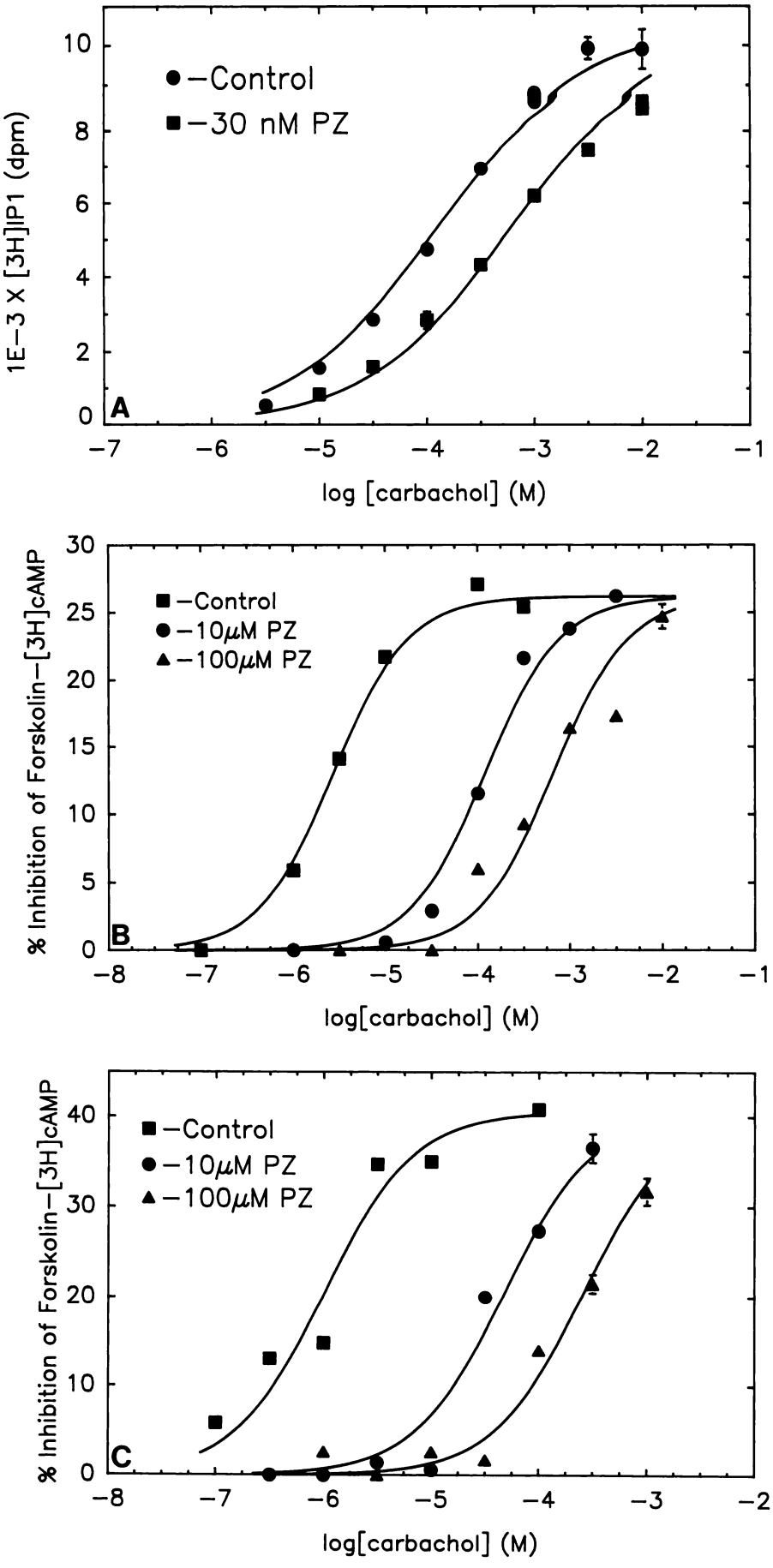

Fig. 2. Effect of pirenzepine on carbachol-induced cortical and striatal biochemical responses. A, Effect of 30 nM pirenzepine (*PZ*) on carbachol-mediated phosphoinositide metabolism in dissociated cerebral cortex. This is one of six similar experiments, in which the pirenzepine concentration ranged from 30 nM to 300 nM. B, Effect of 10 μM and 100 μM pirenzepine on carbachol-mediated inhibition of 10 μM forskolin-elevated [^{3}H]cAMP levels dissociated cerebral cortex. This is one of four experiments, each performed in quadruplicate, in which the pirenzepine concentration ranged from 1 μM to 100 μM. C, Effect of 10 μM and 100 μM pirenzepine on carbachol-mediated inhibition of 10 μM forskolin-elevated [^{3}H]cAMP levels in dissociated striatal tissue. This is one of two similar experiments, in which five concentrations of pirenzepine ranging from 1 μM to 100 μM were tested; each experiment was performed in quadruplicate. The legends within the panels indicate the concentrations of pirenzepine used for the experiments shown. The K_d values for the antagonist calculated from the dose ratios are given in the text.

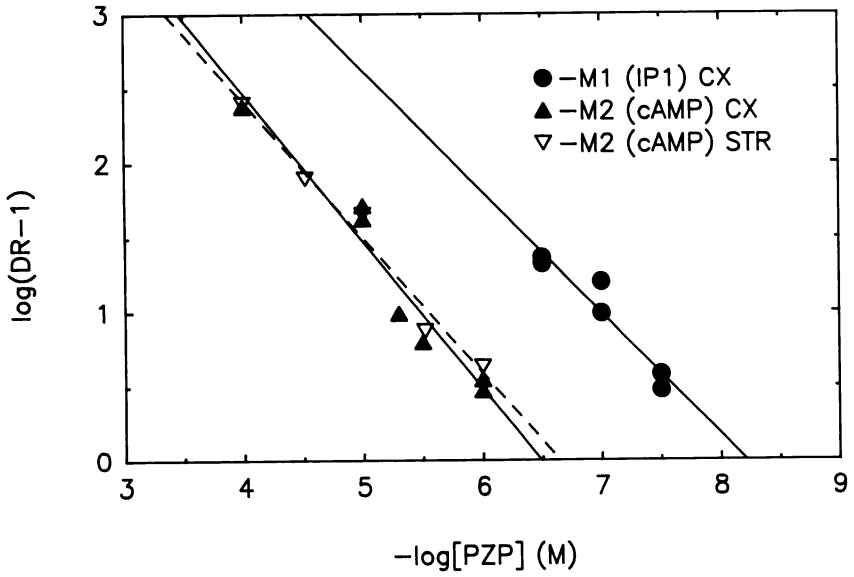

Fig. 3. Schild plots for the blockade of carbachol-induced cortical and striatal second messenger responses to pirenzepine. The dose ratios for experiments of the type shown in Fig. 2 were obtained and plotted by the method of Arunlakshana and Schild. (38). Six experiments with cortical (*CX*) [^{3}H]inositol 1-phosphate formation (●), five experiments with seven concentrations of pirenzepine versus the carbachol-induced cortical [^{3}H]cAMP inhibition response in the cortex (▲), and two experiments with five pirenzepine concentrations versus carbachol-induced [^{3}H]cAMP inhibition in the striatum (*STR*) (▽ – – –) are plotted. The slopes of the plots were 0.89 ± 0.12, 0.99 ± 0.11, and 0.91 ± 0.08 for these three plots, respectively. These slopes were not significantly different from unity; therefore the data in this figure were constrained to unit slope and the resulting p*A*2 values are given in Table 1.

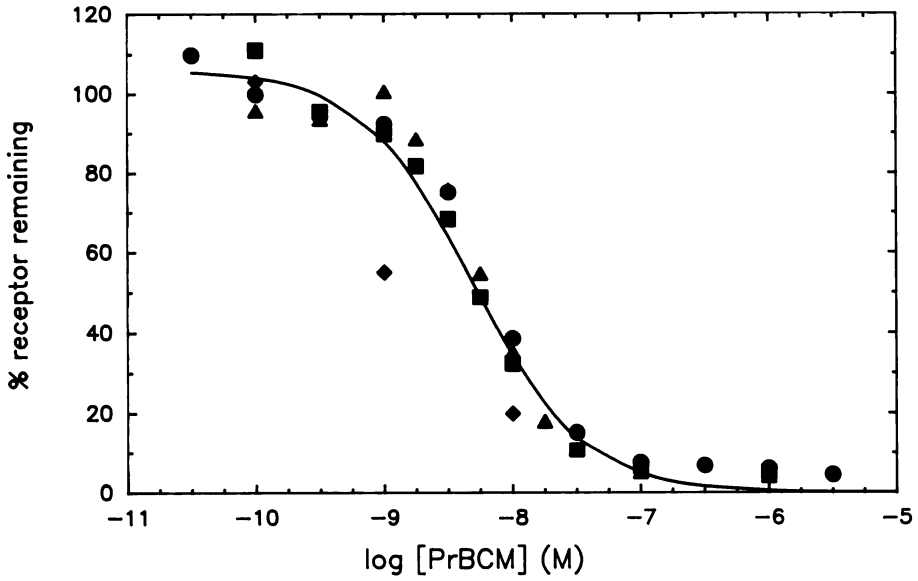

Fig. 4. Occlusion of [^{3}H]*N*-methylscopolamine binding sites in dissociated cortical tissue by 20-min incubation with varying concentrations of PrBCM. Alkylated tissue was washed twice before binding with 1 nM [^{3}H]*N*-methylscopolamine was performed at room temperature for 1 hr. This figure is a composite of four experiments; results from each experiment are shown with the various symbols. The concentration of PrBCM that caused half-maximal blockade of binding was 5.6 nM.

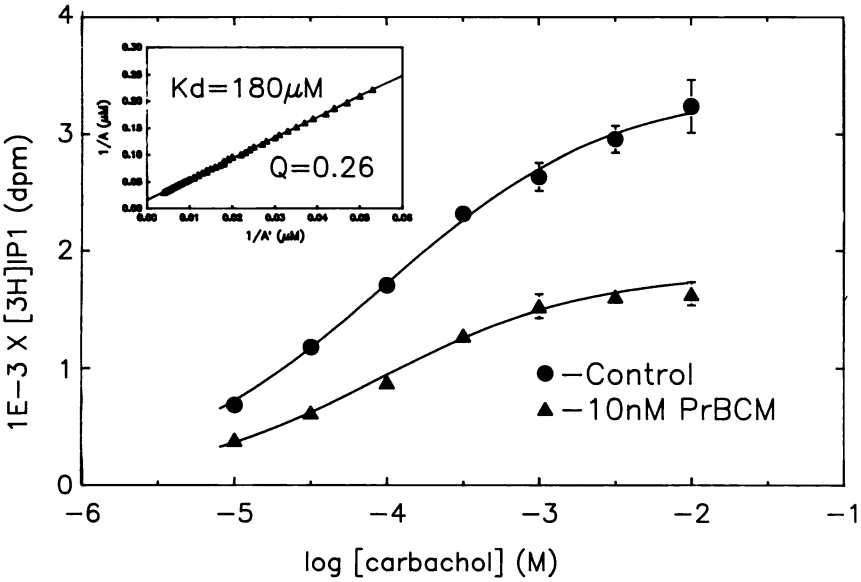

Fig. 5. Effect of alkylation of cortical muscarinic receptors on the concentration-response relation of carbachol for the M1-mediated phosphoinositide response ([^{3}H]inositol 1-phosphate formation) in dissociated cortical tissue. The *inset* shows the K_d for carbachol and the *Q* value (fraction of unoccluded receptors), calculated as described in Methods and Ref. 35. This is one of five similar experiments, each performed in triplicate, which are summarized in Table 2.

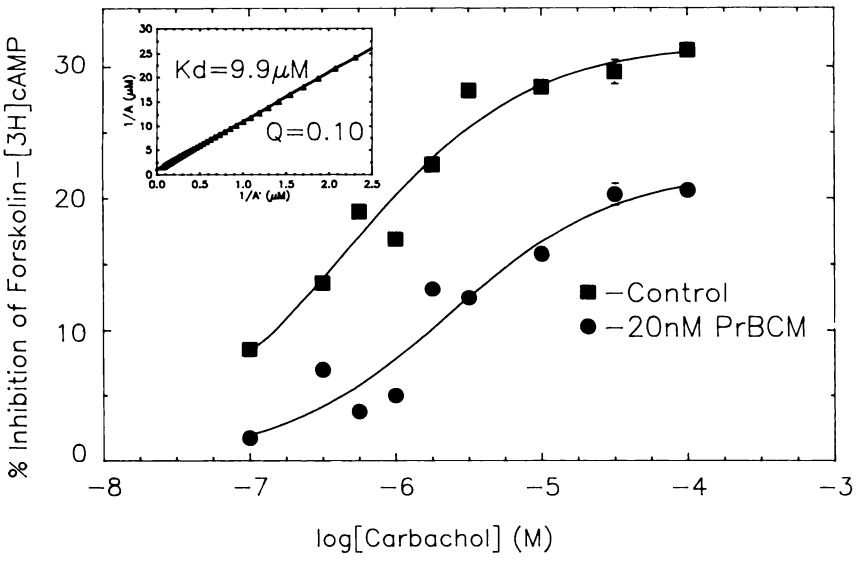

Fig. 6. Effect of alkylation of cortical muscarinic receptors with 20 nM PrBCM on the M2-mediated [^{3}H]cAMP inhibition response in dissociated cerebral cortex. The K_d for carbachol and the Q value (fraction of unoccluded receptors) were calculated as described in Methods and are shown in the *inset*, which is a plot of the inverse of the equieffective concentrations of carbachol (35). This is one of three experiments, each performed in quadruplicate, which are summarized in Table 2.

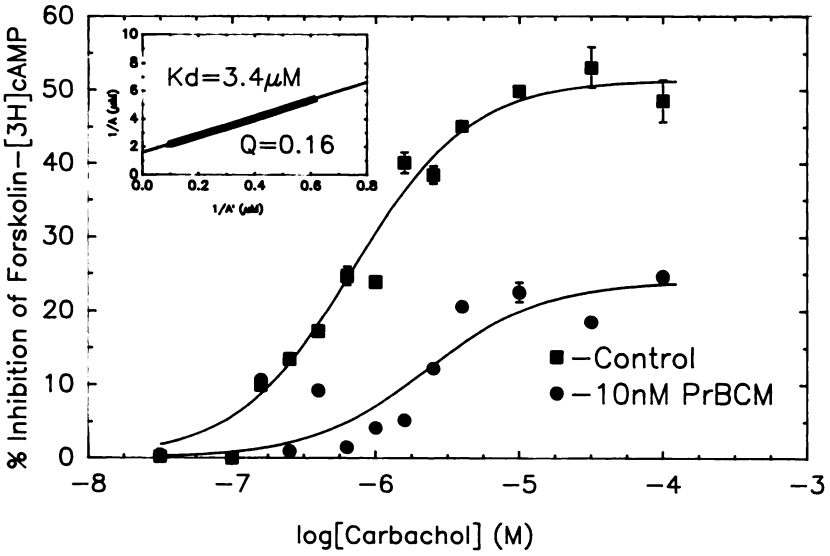

Fig. 7. Effect of alkylation of striatal muscarinic receptors with 10 nM PrBCM on the M2-mediated [^{3}H]cAMP inhibition response in striatum. The K_d for carbachol and the Q value (proportion of unoccluded receptors) for the experiment were calculated as described in Methods (35) and are shown in the *inset*. This is one of five experiments, each performed in quadruplicate. The data for all experiments are summarized in the text and in Table 2.

TABLE 2

Determination of the dissociation constants for carbachol in M1 and M2 muscarinic receptor-mediated biochemical responses in dissociated cortex and striatum

Values were determined in experiments in which treatment with PrBCM was employed to partially occlude receptors. The EC_{50} and maximum response values are for the control (untreated) curves, whereas the K_d values were determined by comparing control and treated curves by the method of Furchgott and Bursztyn (35). Numbers in parentheses, number of experiments.

Parameter	Cortex		Striatum, M2-cAMP
	M1-Inositol 1-phosphate	M2-cAMP	
EC_{50} Control (μM)	100 ± 7 (5)	0.9 ± 0.1[a] (5)	0.9 ± 0.04[a] (4)
Maximal response, control	6.4 ± 0.6 fold[b] (5)	28 ± 1.7% inhibition (5)	48.5 ± 1.3% inhibition (4)
K_d carbachol (μM)	90 ± 11 (5)	8.5 ± 3.1[c,d] (3)	2.9 ± 0.6[e,f] (5)

[a] Significantly different from M1-inositol 1-phosphate EC_{50}, $p < 0.001$.
[b] Refers to the maximal formation over basal levels of [^{3}H]inositol 1-phosphate in stimulated control tissue; basal levels were 567 ± 64 dpm (five experiments).
[c] Significantly different from M1-inositol 1-phosphate K_d, $p < 0.05$.
[d] Significantly different from cortex M2-cAMP EC_{50}, $p < 0.05$.
[e] Significantly different from M1-inositol 1-phosphate K_d, $p < 0.001$.
[f] Significantly different from striatal M2-cAMP EC_{50}, $p < 0.05$.

ment of ligand selectivities. That this is a valid point is shown by the fact that amitriptyline is nonselective when comparing its antimuscarinic potencies at M1 and M2 receptors in dissociated cortex in this fashion (29), whereas the antidepressant appears to be M2 selective when the comparison is made using different types of tissue preparations for the M1 and M2 assay (39). It is, thus, likely that the 3-fold M1 selectivity for atropine found in the present study is real.

Although the M1 receptor predominates in cerebral cortex, a subpopulation of binding sites with low affinity for pirenzepine is also present (40, 41), and functional data indicate that these are coupled to cAMP inhibition (23) and modulation of acetylcholine release (24, 25). From one binding study (42), it appears that two cortical M2 receptors exist, one being similar to the cardiac M2 receptor (judging by the potency of AFDX 116) and the other appearing similar to the ileal M2 receptor (judging by the potency of 4-diphenylacetoxy-*N*-methyl-piperidine methbromide). However, molecular biological studies indicate that only M1, M3, and M4 muscarinic receptors are expressed in cortex (5). Therefore, the cortical M2 receptors identifiable by cAMP inhibition or by modulation of acetylcholine release may reside on terminals of ascending cholinergic (or noncholinergic) projections. The cortical M2 receptors that modulate acetylcholine release and inhibit cAMP have not been characterized sufficiently to compare them either with each other or with smooth muscle, cardiac, or glandular M2 receptors. Striatal M2 receptors are also linked to cAMP metabolism (18, 23) and the modulation of acetylcholine release (24, 25). Thus, it might be speculated that cAMP metabolism is involved in M2-mediated presynaptic inhibition of acetylcholine release in cortex and striatum, whereas the cortical M1-mediated phosphoinositide metabolic response may underly postsynaptic excitation (7, 20) or long term potentiation (43).

The differential binding of agonists to M1 and M2 receptors, found in our functional studies, may help to explain the reported correlation between high affinity binding sites for pirenzepine (M1 receptors) and low affinity binding sites for carbachol in various brain regions (41), inasmuch as the dissociation constant for carbachol (90 μM), determined at a pharmacologically defined M1 receptor, is quite similar to the low affinity binding constant for this agonist measured in cortical membranes (66 μM) (44). However, the dissociation constants for carbachol at M2 receptors (8.5 μM and 3 μM) are somewhat larger than the high affinity binding constant for carbachol in cortical membranes (44). This discrepancy may reflect the involvement of guanine-nucleotide binding proteins, which seem to regulate M2 receptors (45) more than M1 receptors (46). It might be expected that, in a metabolically active preparation such as the dissociated cortex or striatum used in our studies, the level of GTP would be higher than in membranes derived from the brain.

In the present study with brain tissue, as well as in a previous study with N1E-115 mouse neuroblastoma cells (47), we found that carbachol is bound to the M1 receptor in a low affinity active conformation whereas this agonist is bound to the M2 receptor in a high affinity active conformation. Thus, our data indicate a fundamental difference in the recognition of agonists by M1 and M2 receptors. One possible explanation for this phenomenon may relate to differing protein structures for M1 and M2 receptors. It is noteworthy that, in transfection experiments with human muscarinic genes, in which all four subtypes display multiple states for the binding of carbachol, the M1 muscarinic receptor displays much lower affinities for both binding states for carbachol than the corresponding states of the M2 receptor (6). However, the interaction of the receptor with the effector is probably also important in determining the potency with which the agonist binds.

The fact that agonists bind with higher potency to M2 receptors (activation of which is thought to inhibit cholinergic tone) than to cortical M1 receptors (activation of which is important in cognition) sets limits on the selectivity of ligands that may be employed to manipulate cholinergic systems. Additionally important is the fact that M2 receptors are more efficiently coupled than the cortical M1 receptor. If *in vivo* effects can be predicted from these *in vitro* properties, it would appear that the behavioral profile of partial muscarinic agonists will reflect more their activity at M2 receptors than that at M1 receptors and that M2-mediated side effects will be pronounced in agonist therapy with nonselective agonists.

References

1. Kubo, T., K. Fukuda, A. Mikami, A. Maeda, H. Takahashi, M. Mishina, T. Haga, K. Haga, A. Ichiyama, K. Kangawa, M. Kojima, H. Matsuo, T. Hirose, and S. Numa. Cloning, sequencing and expression of complementary DNA encoding the muscarinic acetylcholine receptor. *Nature (Lond.)* **323**:411–416 (1986).
2. Kubo, T., A. Maeda, K. Sugimoto, I. Akiba, A. Mikami, H. Takahashi, T. Haga, K. Haga, A. Ichiyama, K. Kangawa, H. Matsuo, T. Hirose, and S. Numa. Primary structure of porcine cardiac muscarinic acetylcholine receptor deduced from the cDNA sequence. *FEBS Lett.* **209**:367–372 (1986).
3. Peralta, E. G., J. W. Winslow, G. L. Peterson, D. H. Smith, A. Ashkenzai, J. Ramachandran, M. I. Schimerlik, and D. J. Capon. Primary structure and biochemical properties of an M2 muscarinic receptor. *Science (Wash. D. C.* **236**:600–605 (1987).
4. Braun, T., P. R. Schofield, B. D. Shivers, D. B. Prichett, and P. H. Seeburg. A novel subtype of muscarinic receptor identified by homology screening. *Biochem. Biophys. Res. Commun.* **149**:125–132 (1987).
5. Bonner, T. I., N. J. Buckley, A. C. Young, and M. R. Brann. Identification of a family of muscarinic acetylcholine receptor genes. *Science (Wash. D. C.)* **237**:527–532 (1987).
6. Peralta, E. G., A. Ashkenazi, J. W. Winslow, D. H. Smith, J. Ramachandran, and D. J. Capon. Distinct primary structures, ligand-binding properties and tissue-specific expression of four human muscarinic acetylcholine receptors. *EMBO J.* **6**:3923–3929 (1987).
7. Krnjevic, K., and J. W. Phillis. Acetylcholine-sensitive cells in the cerebral cortex. *J. Physiol. (Lond.)* **166**:296–327 (1963).
8. Sillito, A. M., and J. A. Kemp. Cholinergic modulation of the functional organization of the cat visual cortex. *Brain Res.* **289**:143–155 (1983).
9. Donoghue, J. P., and K. L. Carroll. Cholinergic modulation of sensory responses in rat primary somatosensory cortex. *Brain Res.* **408**:367–371 (1987).
10. Inoue, M., Y. Oomura, H. Nishino, S. Aou, S. Sikdar, M. Hynes, Y. Mizuno, and T. Katabuchi. Cholinergic role in monkey dorsolateral prefrontal cortex during bar-press feeding behavior. *Brain Res.* **278**:185–194 (1983).
11. Fukuchi, I., S. Kato, M. Nakahiro, S. Uchida, R. Ishida, and H. Yoshida. Blockade of cholinergic receptors by an irreversible antagonist, propylbenzilylcholine mustard (PrBCM), in the rat cerebral cortex causes deficits in passive avoidance learning. *Brain Res.* **400**:53–61 (1987).
12. Rigdon, G. C., and J. H. Pirch. Nucleus basalis involvement in conditioned neuronal responses in the rat frontal cortex. *J. Neurosci.* **6**:2535–2542 (1986).
13. Johnston, M. V., M. McKinney, and J. T. Coyle. Evidence for a cholinergic projection to neocortex from neurons in the basal forebrain. *Proc. Natl. Acad. Sci. USA* **76**:5392–5396 (1979).
14. Irle, E., and H. J. Markowitsch. Basal forebrain-lesioned monkeys are severely impaired in tasks of association and recognition memory. *Ann. Neurol.* **22**:735–743 (1987).
15. Caulfield, M. P., G. A. Higgins, and D. W. Straughan. Central administration of the muscarinic receptor subtype-selective antagonist pirenzepine selectively impairs passive avoidance learning in the mouse. *J. Pharm. Pharmacol.* **35**:131–132 (1983).
16. Hagan, J. J., J. H. M. Jansen, and C. L. E. Broekkamp. Blockade of spatial learning by the M1 muscarinic antagonist pirenzepine. *Psychopharmacology* **93**:470–476 (1987).
17. Messer, W. S., G. J. Thomas, and W. Hoss. Selectivity of pirenzepine in the central nervous system. II. Differential effects of pirenzepine and scopolamine on performance of a representational memory task. *Brain Res.* **407**:37–45 (1987).
18. Gil, D. W., and B. B. Wolfe. Pirenzepine distinguishes between muscarinic

receptor-mediated phosphoinositide breakdown and inhibition of adenylate cyclase. *J. Pharmacol. Exp. Ther.* **232**:608–616 (1985).
19. Fisher, S. K., and R. T. Bartus. Regional differences in the coupling of muscarinic receptors to inositol phospholipid hydrolysis in guinea pig brain. *J. Neurochem* **45**:1085–1095 (1985).
20. McCormick, D. A., and D. A. Prince. Two types of muscarinic response to acetylcholine in mammalian cortical neurons. *Proc. Natl. Acad. Sci. USA* **82**:6344–6348 (1985).
21. Worley, P. F., J. M. Baraban, M. McCarren, S. H. Snyder, and B. E. Alger. Cholinergic phosphatidylinositol modulation of inhibitory, G protein-linked, neurotransmitter actions: electrophysiological studies in rat hippocampus. *Proc. Natl. Acad. Sci. USA* **83**:3467–3471 (1987).
22. Dutar, P., and R. A. Nicoll. Stimulation of phosphatidylinositol (PI) turnover may mediate the muscarinic suppression of the M-current in hippocampal pyramidal cells. *Neurosci. Lett.* **85**:89–94 (1988).
23. Anderson, D. J., and M. McKinney. Muscarinic M2 receptor-mediated cyclic AMP reduction in mechanically dissociated rat cortex. *Brain Res.*, in press.
24. Raiteri, M., R. Leardi, and M. Marchi. Heterogeneity of presynaptic muscarinic receptors regulating neurotransmitter release in the rat brain. *J. Pharmacol. Exp. Ther.* **228**:209–214 (1984).
25. Meyer, E. M., and D. H. Otero. Pharmacological and ionic characterization of the muscarinic receptors modulating [^{3}H]acetylcholine release from rat cortical synaptosomes. *J. Neurosci.* **5**:1202–1207 (1985).
26. Olianas, M. C., P. Onali, N. H. Neff, and E. Costa. Adenylate cyclase activity of synaptic membranes from rat striatum: inhibition by muscarinic receptor agonists. *Mol. Pharmacol.* **23**:393–398 (1983).
27. Fisher, S. K., and R. M. Snider. Differential receptor occupancy requirements for cholinergic stimulation of inositol lipid hydrolysis in brain and in neuroblastomas. *Mol. Pharmacol.* **32**:81–90 (1987).
28. McKinney, M., S. Stenstrom, and E. Richelson. Muscarinic responses and binding in a murine neuroblastoma clone (N1E-115): mediation of separate responses by high affinity and low affinity agonist-receptor conformations. *Mol. Pharmacol.* **27**:223–235 (1985).
29. McKinney, M., N. H. Lee, D. J. Anderson, L. Vella-Rountree, and E. E. El-Fakahany. Nonselectivity of amitriptyline for subtypes of brain muscarinic receptors demonstrated in binding and functional assays. *Eur. J. Pharmacol.*, in press.
30. Honnegger, P., and E. Richelson. Biochemical differentiation of mechanically dissociated mammalian brain in aggregating cell culture. *Brain Res.* **109**:335–354 (1976).
31. Kanba, S., and E. Richelson. Antidepressants are weak competitive antagonists of histamine H2 receptors in dissociated brain tissue. *Eur. J. Pharmacol.* **94**:313–354 (1983).
32. El-Fakahany, E., and J.-H. Lee. Agonist-induced acetylcholine receptor down-regulation in intact rat brain cells. *Eur. J. Pharmacol.* **132**:21–30 (1986).
33. Lin, C. W., B. R. Bianchi, D. Grant, T. Miller, E. A. Danaher, M. D. Tufano, H. Kopecka, and A. M. Nadzan. Cholecystokinin receptors: relationships among phosphoinositide breakdown, amylase release and receptor affinity in pancreas. *J. Pharmacol. Exp. Ther.* **236**:729–734 (1986).
34. DeLean, A., P. J. Munson, and D. Rodbard. Simultaneous analysis of families of sigmoidal curves: application to bioassay, radioligand assay, and physiological dose-response curves. *Am. J. Physiol.* **235**:E97–E102 (1978).
35. Furchgott, R. F., and P. Bursztyn. Comparison of dissociation constants and of relative efficacies of selected agonists acting on parasympathetic receptors. *Ann. N. Y. Acad. Sci.* **144**:882–899 (1967).
36. Fleming, W. W., D. P. Westfall, I. S. De La Lande, and L. B. Jellett. Log-normal distribution of equieffective doses of norepinephrine and acetylcholine in several tissues. *J. Pharmacol. Exp. Ther.* **181**:339–345 (1972).
37. De Lean, A., A. A. Hancock, and R. J. Lefkowitz. Validation and statistical analysis of a computer modeling method for quantitative analysis of radioligand binding data for mixtures of pharmacological receptor subtypes. *Mol. Pharmacol.* **21**:5–16 (1982).
38. Arunlakshana, O., and H. O. Schild. Some quantitative uses of drug antagonists. *Br. J. Pharmacol.* **14**:48–58 (1959).
39. Nomura, S., S. H. Zorn, and S. J. Enna. Selective interaction of tricyclic antidepressants with a subclass of rat brain cholinergic muscarinic receptors. *Life Sci.* **40**:1751–1760 (1987).
40. Luthin, G. R., and B. B. Wolfe. Comparison of [^{3}H]pirenzepine and [^{3}H] quinuclidinylbenzilate binding to muscarinic cholinergic receptors in rat brain. *J. Pharmacol. Exp. Ther.* **228**:648–655 (1984).
41. Cortes, R., and J. M. Palacios. Muscarinic cholinergic receptor subtypes in the rat brain. I. Quantitative autoradiographic studies. *Brain Res.* **362**:227–238 (1986).
42. Waelbroeck, M., M. Gillard, P. Robberecht, and J. Christophe. Muscarinic receptor heterogeneity in rat central nervous system. I. Binding of four selective antagonists to three muscarinic receptor subclasses: a comparison with M2 cardiac muscarinic receptors of the C type. *Mol. Pharmacol.* **32**:91–99 (1987).
43. Metherate, R., N. Tremblay, and R. W. Dykes. Acetylcholine permits long-term enhancement of neuronal responsiveness in cat primary somatosensory cortex. *Neuroscience* **22**:75–81 (1987).
44. McKinney, M., and J. T. Coyle. Regulation of neocortical muscarinic receptors: effects of drug treatment and lesions. *J. Neurosci.* **2**:97–105 (1982).
45. Sokolovsky, M., D. Gurwitz, and R. Galron. Muscarinic receptor binding in mouse brain: regulation by guanine nucleotides. *Biochem. Biophys. Res. Commun.* **94**:487–492 (1980).
46. Watson, M., H. I. Yamamura, and W. R. Roeske. [^{3}H]Pirenzepine and (−)-quinuclidinyl benzilate binding to rat cerebral cortical and cardiac muscarinic cholinergic sites. I. Characterization and regulation of agonist binding to putative muscarinic subtypes. *J. Pharmacol. Exp. Ther.* **237**:411–418 (1986).
47. McKinney, M., and E. Richelson. Muscarinic responses and binding in a murine neuroblastoma clone (N1E-115): cyclic GMP formation is mediated by a low affinity agonist-receptor conformation and cyclic AMP reduction is mediated by a high affinity agonist-receptor conformation. *Mol. Pharmacol.* **30**:207–211 (1986).

Send reprint requests to: M. McKinney, Neuroscience Research Division, Pharmaceutical Discovery, Dept. 47W, Abbott Laboratories, Abbott, IL 60064.